6.2 'Implicit' coupling algorithm - FSI problems with finite deformations for the structural part

To demonstrate the implicit coupling algorithm presented in section 5.5, the laminar flow around an elastic cylinder will be investigated.

The two-dimensional flow around a rigid cylinder has been well studied experimentally as well as numerically. A very good overview can be found in [51]. For these disturbance-free flows the main *governing* parameter is the Reynolds number Re. Following [51] three regimes are distinguished in the case of a laminar flow:

• No-separation regime for Re between 0 and 4–5.

• Closed wake regime for Re between 4–5 and 30–48. In this case a distinct, steady, symmetric, and closed near-wake is formed behind the cylinder.

• Periodic wake regime for Re between 30–48 and 180–200. This flow regime is characterised by the development of a periodic vortex street famous by the name Karman-Bernard vortex street.

However, the real case three-dimensional flows can be also affected by a number of *influencing* parameters: turbulence, surface roughness, wall blockage, aspect ratio, cylinder oscillations.

There are numbers of studies about rigid cylinders oscillating perpendicularly to the flow direction for example [7], [25] and [40]. However, if the cylinder is elastic there are very few experimental and numerical results.

Therefore, it is interesting to study the flow pattern when the cylinder is made of an elastic material. A configuration similar to the one used in [49] is taken. The cylinder has a diameter d = 0.006 m. It is placed in the middle of the fluid domain, at distance 6d from the inlet. The computational domain is chosen to have width 12d and length d. The outlet boundary is chosen 25d behind the cylinder so that it does not affect the flow behaviour around the body. On the rest of the boundaries symmetry boundary conditions are applied. The schematic problem description is given in Figure 6.11.

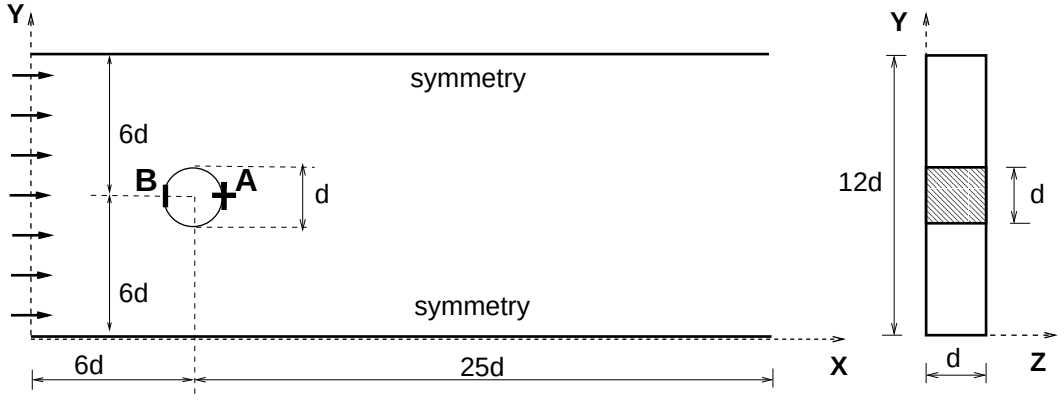

Figure 6.11: Flow around cylinder - geometry description

The fluid has density $\rho_{fluid} = 1180$ kg/m^3 and viscosity $\mu = 0.0182$ Pa/s. Its velocity at the inlet has a block profile with a bulk velocity v_0.Obviously, if the fluid properties are fixed, the Reynolds number

$$\mathrm{Re} = \frac{\mathrm{d}\ v_0\ \rho_{fluid}}{\mu}$$

depends on the bulk velocity.

To study the different flow regimes, the following cases will be considered:

• Case 1: Re = 20, i.e. a steady-state laminar flow. In this case the bulk velocity is chosen $v_0 = 0.05$ m/s.

• Case 2: Re = 100, i.e. a periodic state laminar flow. The corresponding bulk velocity is $v_0 = 0.25$ m/s.

The structural parameters are different in the both cases and will be additionally given. However, the same boundary conditions are applied on the structure. The cylinder is assumed to be fixed at the point A and to move only horizontally at the point B, see Figure 6.11. Its thickness is d/20, i.e. 3.E-04 m. To allow finite deformations, an elastic energy conserving material law is chosen.

Additionally, the pressure at the outlet is fixed to be equal to the static pressure, which is the same as the pressure inside the cylinder.

To solve the fluid dynamics subproblem the fluid domain is discretised into a finite volume block-structured grid consisting of three blocks. Let us notice that only the grid-block containing the elastic cylinder has to be modified to fit the new cylinder position.

Due to the symmetry conditions on the top and the bottom of the domain, the fluid forces acting on the cylinder are constant along the cylinder, i.e. in z-direction. Moreover, the z-components of these forces can be neglected and the structural problem may be solved as two-dimensional. Therefore, only a part of the cylinder with a length equal to the grid-spacing along z-axis is considered by the structural problem. The cylinder is discretised into beam elements, i.e. 2-node finite elements with 4 degrees of freedom (2 translations and 2 rotations).

The fluid-structure interaction between the flow and the cylinder is simulated by the implicit coupling algorithm of a predictor-corrector type. In this way the equilibrium between flow and structure is found at every time-step. The Crank-Nicolson time-discretisation scheme is applied within the fluid solver. To have a consistent time-discretisation, for the structural program the conserving form of the α-method is selected.

6.2.1 Case 1: Laminar flow around an elastic cylinder (Re = 20)

As it was already mentioned in this case the fluid bulk velocity is 0.05 m/s, which corresponds to Reynolds number 20 for a rigid cylinder. The cylinder is made of an

isotropic elastic conserving material with Young modulus $E = 722$ N/m^2, Poisson ratio $\nu = 0.4$ and density $\rho_{struc} = 2000$ kg/m^3.

In the beginning of the simulation the flow is taken to be the steady state laminar flow around the rigid cylinder. The start horizontal velocity and streamtraces are presented in Figure 6.12 (left). A symmetric steady wake appears behind the body. Its length L_w is approximately equal to the diameter d. This is in accordance with the empirical formula $L_w = 0.05$ d Re [51], that gives $L_w =$ d for Re $= 20$.

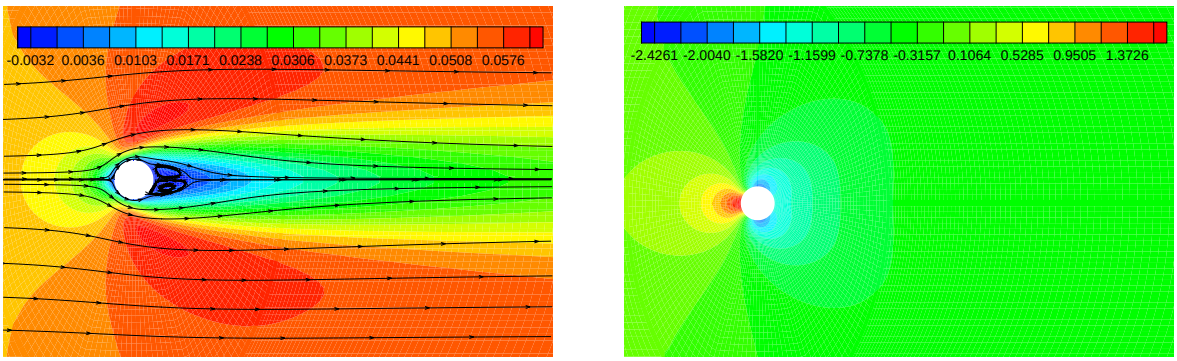

Figure 6.12: Flow around rigid cylinder at Re $= 20$ - steady state: Horizontal velocity and streamtraces (left) and pressure distribution (right)

Special attention deserves the pressure distribution around the cylinder presented in Figure 6.12 (right). There are a high pressure in front (at point B) and two areas of low pressure on the two sides of the cylinder. Hence, it is expected that if the cylinder is elastic it will mainly deform due to the high front pressure.

The fluid behaviour when fluid-structure interaction is taken into account is investigated time-dependently. In order to prevent instabilities due to bad starting conditions, the fluid forces are underrelaxed. Additionally, step 0.01 s is chosen for time discretisation.

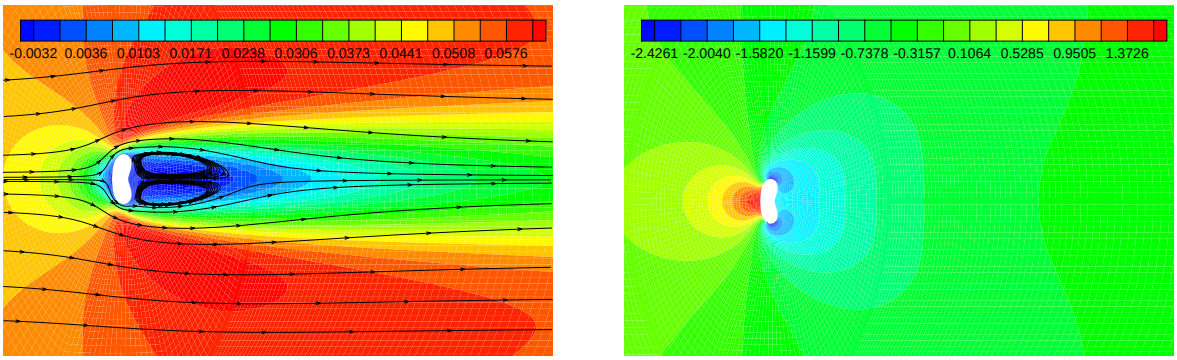

Figure 6.13: Flow around elastic cylinder at Re $= 20$ - steady state: Horizontal velocity and streamtraces (left) and pressure distribution (right)

In the beginning of the simulation the cylinder starts oscillating due to the fluid forces. Simultaneously, the flow field and pressure are also affected. Eventually, a steady state

between the flow and the structure is reached. The obtained equilibrium is presented in Figure 6.13, where the horizontal velocity and streamtraces are depicted on the left and the pressure distribution on the right.

As it was expected the biggest structural deformation is at the point B. The comparison with the flow field around a rigid cylinder shows that the closed wake behind the elastic cylinder is about 2.5 times bigger. This is a result of the changed shape of the cylinder.

With regard to the predictor-corrector scheme, in the beginning of the simulation typically 15 predictor-corrector iterations per time-step have been necessary to obtain fluid-structure equilibrium. The number of iterations reduces as the steady state is approached and finally, just one iteration per time-step is enough.

6.2.2 Case 2: Laminar flow around an elastic cylinder (Re = 100)

Before taking into account the interaction between the flow and the elastic cylinder, let us firstly consider the flow around a rigid cylinder.

The fluid bulk velocity is chosen to be $v_0 = 0.25$ m/s so that the Reynolds number is 100. The flow is investigated time-dependently using time-step 0.004 s. The obtained flow pattern, well known as Karman-vortex street, is presented in Figure 6.14.

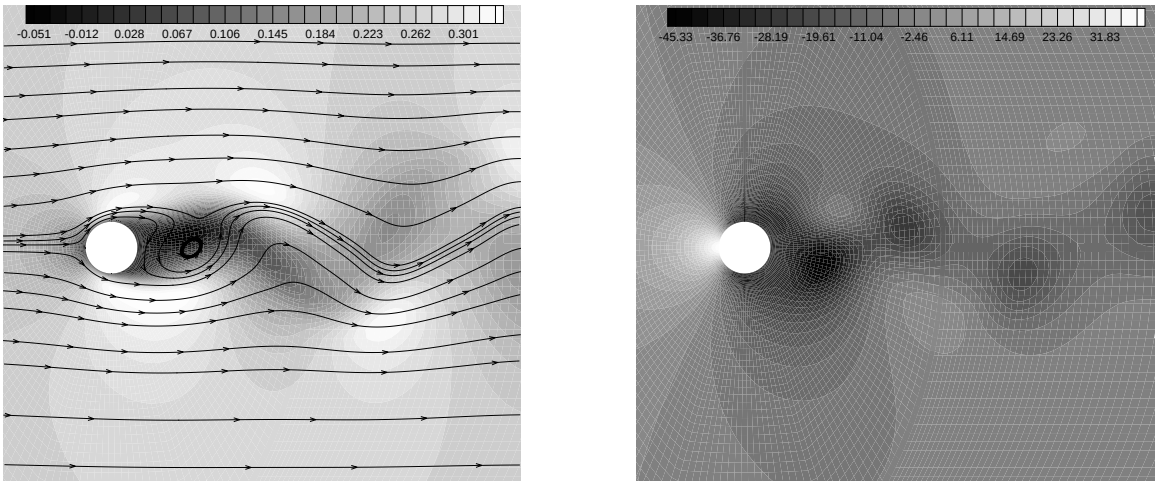

Figure 6.14: Flow around rigid cylinder (Re=100): Horizontal velocity and streamtraces (left) and pressure (right)

The periodic flow leads to a time-variation of the fluid-dynamic force exerted upon the cylinder. This force can be separated into the resultant forces along and perpendicular to the free stream velocity named in the aeroelasticity as a drag and a lift force, respectively. The total fluid-dynamic force depends on the dynamic pressure and the projected area of the cylinder exposed to the free stream. Hence, the drag and lift forces may be reduced to non-dimensional drag C_D and lift C_L coefficients. The last are important parameters of the flow around a cylinder and are defined by:

$$C_D = \frac{F_x}{\frac{1}{2}\rho v_0^2 \, dL} \, , \qquad C_L = \frac{F_y}{\frac{1}{2}\rho v_0^2 \, dL} \, , \tag{6.1}$$

where F_x and F_y are respectively the resultant forces along and perpendicular to the stream direction. The term $\frac{1}{2}\rho v_0^2$ is the dynamic pressure for a flow with a density ρ and bulk velocity v_0. The diameter and the length of the cylinder are denoted with d and L, respectively.

The obtained drag and lift coefficients for the considered flow are depicted in Figure 6.15. The lift coefficient oscillates with a period $T_L = 0.14$ s, that is twice bigger than

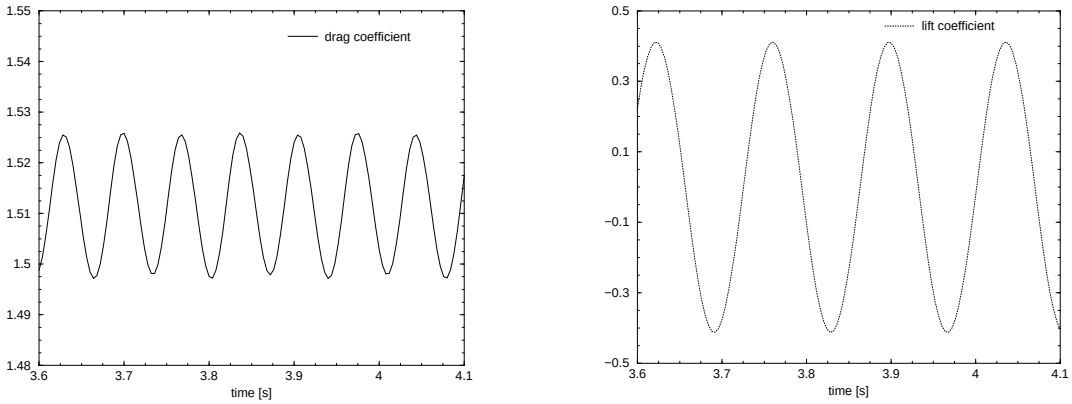

Figure 6.15: Flow around rigid cylinder (Re = 100): Drag (left) and lift (right) coefficients

the period of the drag coefficient. Hence, the Strouhal number St based on T_L is

$$St = \frac{d}{v_0 T_L} \approx 0.17 \ .$$

This value is consistent with the experimental data given in [51]. Because of the symmetry boundary conditions the lift coefficient is oscillating around zero with amplitude 0.41. On the other hand the drag coefficient oscillates around 1.51 with a much smaller amplitude 0.01. Hence, the fluid dynamic forces acting on the cylinder walls vary periodically in time.

Finally, the fluid-structure interaction will be investigated when the cylinder has elastic walls. At the beginning of the simulation the flow is assumed to be the obtained periodic flow around the rigid cylinder.

The cylinder is made of an elastic isotropic material with density $\rho_{struc} = 8000$ kg/m^3, Young modulus $E = 15000$ N/m^2 and Poisson ratio $\nu = 0.4$.

Responding to the periodic fluid forces, the cylinder also starts deforming periodically. On the other hand the elastic walls deformations lead to a change in the flow behaviour. Using a predictor-corrector scheme, at every time-step the equilibrium between the flow and the structure is obtained. Typically 15 predictor-corrector iterations per time-step are needed.

In Figure 6.16 (right) the time history of the drag and lift coefficients within the first 2.5 s with FSI are shown. In the beginning till time zero their values without considering FSI are given for comparison. The effects of the FSI start at time 0 s.

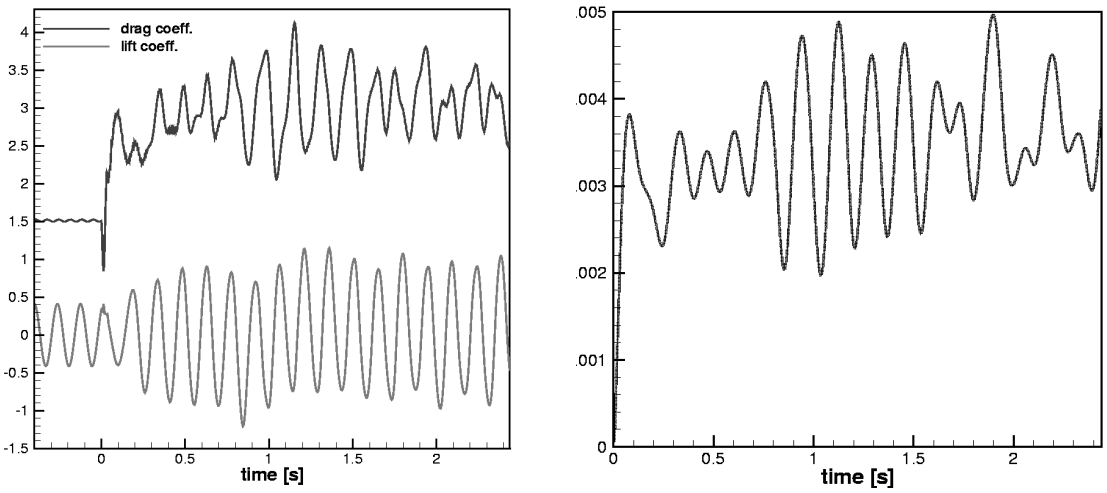

Figure 6.16: Time history of drag and lift coefficients (left) and global displacement at point B (right)

Due to the FSI between the flow and the cylinder both coefficients significantly increase. This can be explained with the change of the cylinder surface exposed to the flow. Despite the different amplitudes, the oscillation periods remain nearly the same.

Since the pressure forces are highest in front of the cylinder, the biggest displacements are observed at the point B. Its global displacement in a horizontal direction is presented in Figure 6.16 (right).

The change in the flow field due to the interaction with the elastic cylinder is presented in Figure 6.17, where the streamtraces and the horizontal velocity at a few selected times are shown. It can be seen that the Karman-vortex street is affected by the elastic walls reaction. The wake behind the cylinder changes its shape as the structure is deformed. The cylinder is oscillating horizontally pressed by the drag force. Due to the elastic walls deformation, the surface exposed to the flow is increased. This leads to a wider wake than the one for the rigid body. Additionally, the velocity reaches bigger maximum and minimum values. As the positive and the negative areas of the horizontal velocity close to the upper and lower parts of the cylinder alternate their positions dynamically, the deformed cylinder is oscillating around the fixed point B.

The time history of both coefficients shows that the magnitude of the dynamic forces acting on the cylinder is varying. As it is expected, the numerical simulation tries to find the equilibrium between the flow and the elastic structure, around which the deformation and the fluid variables are oscillating. However, it turned out that for the chosen elastic material the fluid forces finally lead to a very big deformation at the front point A.

Conclusion

The implicit coupling strategy can be applied successfully to investigate dynamically the fluid-structure interaction of a flow around an elastic cylinder. In Case 1 a steady

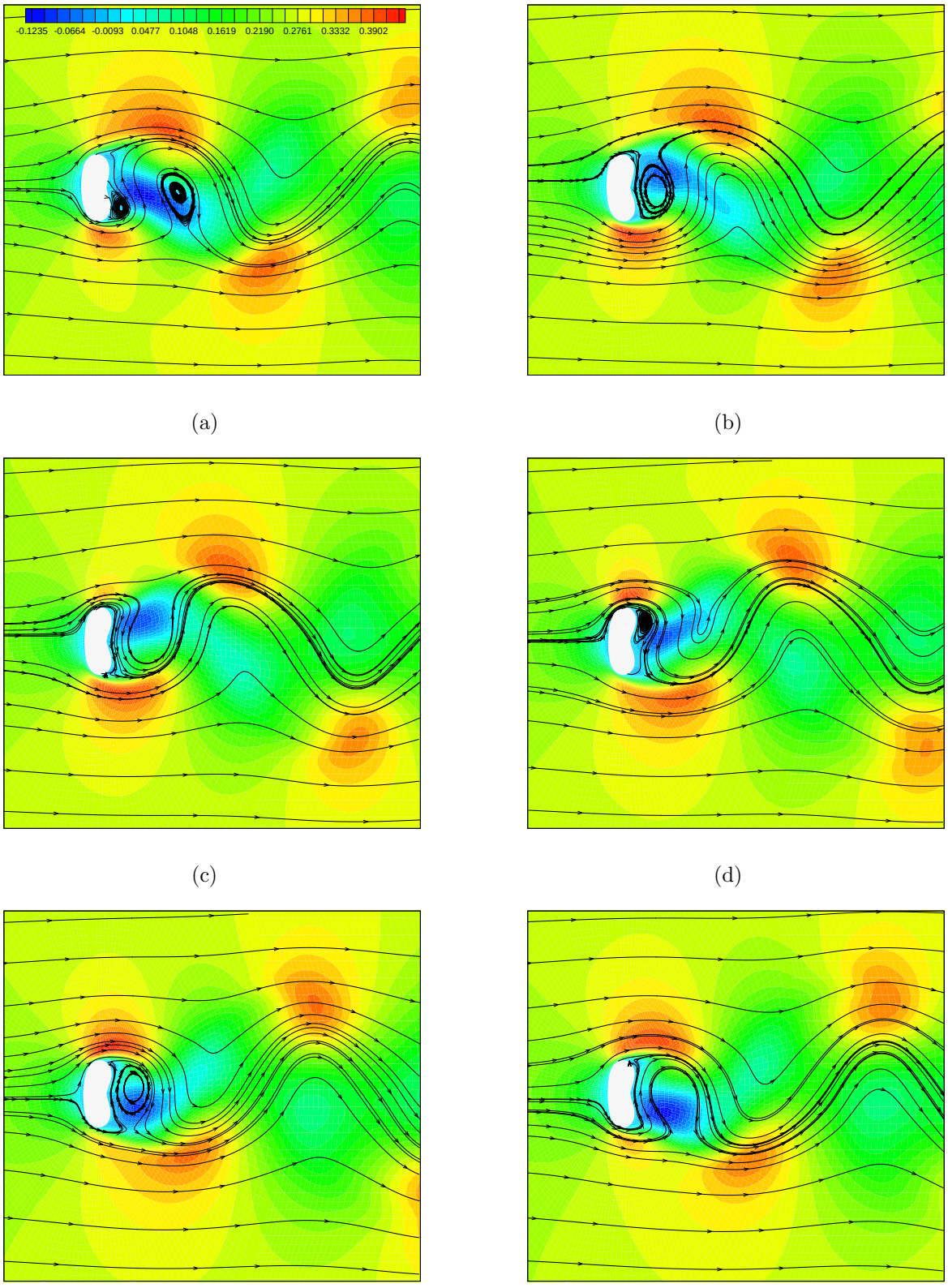

(a) (b)

(c) (d)

(e) (f)

Figure 6.17: Horizontal fluid velocity and streamtraces at different times

state between a flow and a structure has been reached. On the other hand in Case 2 an unsteady non-periodical flow has been received. Due to the rather weak structural material, the fluid forces finally lead to a contact problem for the structural part. In order to solve this contact problem, special methods for the structural solution are needed.